

<i>Cryst. Res. Technol.</i>	<b>34</b>	1999	8	1031–1036
-----------------------------	-----------	------	---	-----------

S.M. KACZMAREK, G. DOMIANIAK-DZIK\*, W. RYBA-ROMANOWSKI\*,  
J. KISIELEWSKI\*\*, J. WOJTKOWSKA\*\*\*

Military University of Technology Warsaw

\*Institute of Low Temperatures and Structure Research PAS Wrocław

\*\*Institute of Electronic Materials Technology (ITME) Warsaw

\*\*\*Soltan Institute of Nuclear Studies (SINS) Swierk, Poland

## Changes in Optical Properties of Ce: YAG Crystals under Annealing and Irradiation Processing

Changes of optical properties of cerium doped YAG single crystals (0.05, 0.1, 0.2 at. % Ce, and 0.2 at. % Ce, 0.1 at. % Mg) after thermal annealing at 1400°C in air or 1200°C in N<sub>2</sub>+H<sub>2</sub> mixture and subsequent  $\gamma$  or proton irradiation were investigated. For initial Ce<sup>3+</sup> contents <0.05 at. % an increase and for Ce<sup>3+</sup> contents >0.05 at. % a decrease of the final Ce<sup>3+</sup> concentration was observed. Appropriate changes in luminescence of Ce: YAG crystals were observed as a consequence of dopant concentration changes. They were small after  $\gamma$ -irradiation of Ce: YAG crystals with Ce<sup>3+</sup> content >0.05at.% and reached about 100% after  $\gamma$ -irradiation of crystals with Ce<sup>3+</sup> content <0.05 at. %.

Keywords: gamma and proton irradiation's, additional absorption, radiation defects, annealing

### 1. Introduction

The Ce<sup>3+</sup>:YAG crystal shows some properties highly desirable for an active material of tuned solid state lasers (TOMKI et al.). The emission band from 4f-5d levels extends from 500 to about 650 nm and has quantum efficiency close to unity. Broad pumping bands exhibit the allowed absorption of the dipole-dipole type. Moreover, the YAG matrix posses excellent thermal and optical properties.

However, a large value of excited state absorption (ESA) excludes a stimulated emission from the excited levels of Ce ions (states 5d) in this material (DEXTER).

The ESA spectrum of Ce<sup>3+</sup>:YAG crystals overlaps with the luminescence spectrum of the trivalent Ce ions. This results in a fast decay of the luminescence (about 60 ns) and thus unable any laser action.

The Ce<sup>3+</sup>:YAG crystal is also used as a scintillator (e.g. in medical imaging, tomography, gamma-cameras) (DEXTER). Parameters of the Ce: YAG crystal as a scintillator and also a potential active medium, to a large extend depends on its optical properties and especially on the kind of the structural and radiation defects. They may emerge in the crystal during the growth process, annealing in high temperatures or irradiation by process (SLACK et al., YEN et al., KACZMAREK et al.).

The main goal of this work was to study those structural and radiation defects which influence the crystal properties qualifying them as scintillator or active laser material.

### 2. Experimental

Single crystals of Ce: YAG and Ce, Mg: YAG were grown by the Czochralski technique in the atmosphere of pure nitrogen in ITME. The growth conditions are described elsewhere (KACZMAREK et al. 1998).

## 2.1 Annealing procedures

Annealing of crystals was done in oxidising and reducing atmospheres. First one at 1400°C in air for 4 hours, performed immediately after the growth process to get rid of the growth defects. The second one, at 1200°C in the gas mixture of N<sub>2</sub>+H<sub>2</sub>, for 0.5 hours, in order to change the defect structure of these crystals.

In order to remove radiation defects, the annealing of Ce: YAG and Ce, Mg: YAG crystals was performed for 3 hours in air at 400°C.

## 2.2 Irradiation conditions

Crystals were irradiated by  $\gamma$ -rays after the growth process (AG), both at room and liquid nitrogen temperatures, and by protons after annealing at 1400°C. The <sup>60</sup>Co  $\gamma$ -source with a strength of 1.5 Gy/sec was used. Samples were irradiated with  $\gamma$ -doses up to 10<sup>5</sup> Gy.

For proton irradiation a beam from C-30 cyclotron of the SINS in  $\bullet$ wierk was used. Proton energy was about 21 MeV, and the beam current at the sample was about 0.2 mA. The proton fluency was varied from 10<sup>13</sup> to 10<sup>16</sup> cm<sup>-2</sup>.

The mean range of 21 MeV protons in a YAG crystal is about 2 mm. Because the thickness of our samples was varying from 1 to 2 mm, each bombarding particle lost part of its initial energy. For example, in the case of 2 mm thick sample, the fluency of 10<sup>13</sup> protons per cm<sup>2</sup> gives the absorbed dose of 36 kGy.

## 2.3 Spectroscopic investigations

From the obtained single crystals, the next fourteen flat-parallel plates, 1 mm thick, were cut and both-side polished: YAG (0.1 at % Ce) (four samples of S1 type), YAG (0.2 at % Ce) (four samples of S2 type), YAG (0.2 at % Ce + 0.1 at. % Mg) (four samples of S3 type) and YAG (0.05 at. % Ce) (two samples of S4 type). Then the optical transmission was measured for all the samples before and after the thermal or radiation treatment: in UV-VIS region by means of a LAMBDA-2 and in the IR region by FTIR-1725 Perkin-Elmer spectrophotometers. For the additional absorption spectra, further labelled as (AA), experimental factor  $\Delta K$  was calculated according to the formula:

$$\Delta K(\lambda) = 1/d \ln ( T_1/T_2 ) \quad (1)$$

where  $\lambda$  is the wavelength,  $d$  is sample thickness,  $T_1$  and  $T_2$  are sample transmissions before and after the treatment process, respectively. The fluorescence spectra were obtained by means of spectrofluorimeter LS-5B of Perkin-Elmer.

## 3. Results and discussion

Figs 1a, b present results of absorption measurements of S2 and S3 samples in the range of 200-600 nm obtained for 300 K and 77 K. As one can see the absorption increases with a decrease of temperature and the characteristic band for 4f-5d transitions with a maximum at 458 nm becomes narrower and more intense.

Fig. 1c shows results of emission measurements in the range of 450-650 nm at 5 K. Measurements performed at room temperature give the same shape of the spectrum (KACZMAREK et al. 1998). Fig. 2a presents changes in absorption spectrum for S1...S4 samples in the range of 200-600 nm obtained after annealing for 3h at 1400°C. Some defects which arise after this process manifest themselves as AA bands with maxima at: 253 nm,

280-310 nm, 338 nm and 458 nm. First band is associated with the presence of non-controlled impurities of  $\text{Fe}^{3+}$  (AKHMADULIN et al.), the second one with non-stoichiometry defects, like  $\text{Ce}^{4+}$  or  $\text{Mg}^{2+}$  ions, third and fourth with changes in cerium concentration. In the IR part of the absorption spectrum the f-f transitions for  $\text{Ce}^{3+}$  ion are seen at about  $4.2 \mu\text{m}$ . A decrease of the absorption values of the two last visible bands is caused by decrease in  $\text{Ce}^{3+}$  concentration, what is obviously an effect of annealing at high temperatures (reaction of the type  $\text{Ce}^{3+} \rightarrow \text{Ce}^{4+}$ ). A band with maximum at  $\sim 280 \text{ nm}$  may also be connected with a recharging process of magnesium ions, what is especially clearly seen for S3 sample.

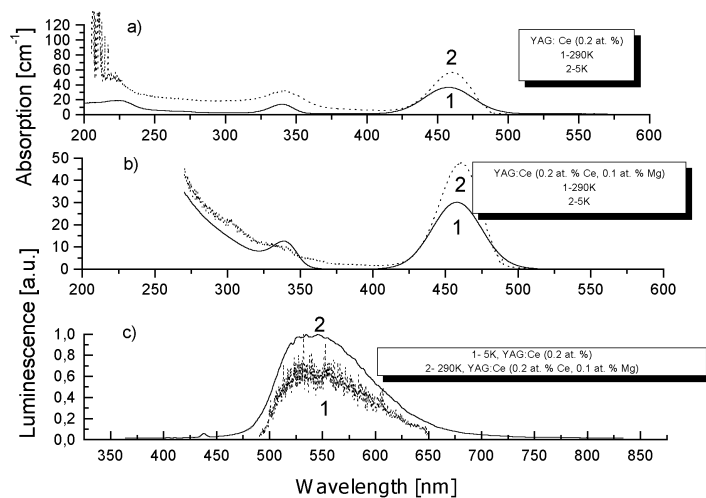


Fig. 1: Absorption at 290K and 77K temperatures for S2 (YAG: Ce 0.2 at. %) and S3 (YAG: Ce 0.2 at. % Ce, 0.1 at. % Mg) samples (a, b) and emission at 5K for S2 and, at 290K for S3 samples (c)

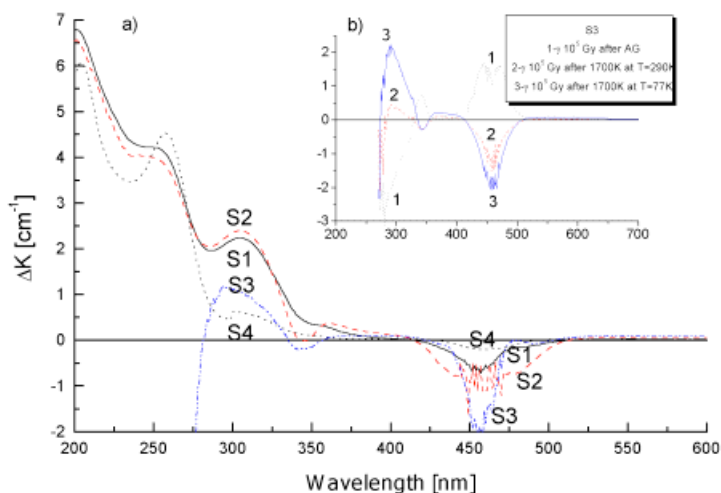


Fig. 2: AA bands for S1(YAG: Ce - 0.1 at. %), S2(YAG: Ce - 0.2 at. %), S3(YAG: Ce, Mg - 0.2 at. % Ce, 0.1 at. % Mg) and S4(YAG: Ce - 0.05 at. %) samples after annealing at 1700K for 3h (a) and after  $10^5$  Gy of S3 sample (b).

Fig. 2b shows changes for S3 sample after subsequent irradiation with  $\gamma$ -rays. After irradiation of „as grown“ S3 sample an increase in final concentration of  $\text{Ce}^{3+}$  ions is seen (curve 1). This is characteristic for Ce: YAG samples with small initial concentration of  $\text{Ce}^{3+}$  ions (e.g. for S4). The presence of magnesium ions in S3 sample favors the presence of some content of  $\text{Ce}^{4+}$  ions. Presence of free electrons emitted during the interaction of  $\gamma$ -rays with

the crystal, (e.g. by Compton effect), leads to the recombination of the  $Ce^{4+}$  to  $Ce^{3+}$  ions. After annealing of the S3 sample at  $1400^{\circ}C$  in air, irradiation with the same value of  $\gamma$  dose, leads to an opposite effect (curve 2). This effect becomes greater after irradiation performed at lower temperature (77K - curve 3). It suggests that during  $\gamma$ -irradiation performed after annealing process, mainly ionization of  $Ce^{3+}$  ions takes place. The same sample irradiated by 21 MeV protons with the fluency of  $10^{14} \text{ cm}^{-2}$  shows the same behavior as described by curve 1. It suggests, that similar recombination processes take place as in the case of Compton effect (this time it probably due to delta electrons produced along the proton trajectory).

Fig. 3a shows AA bands for S1...S3 samples after annealing in  $N_2+H_2$  mixture at  $1200^{\circ}C$  for 0.5 h. One can see clearing in the absorption spectrum in the range where AA bands were previously seen for annealing in the air atmosphere. A decrease in  $Fe^{3+}$  concentration is clearly seen for all samples, a reduction of the defect connected with 310 nm band, and increase in  $Ce^{3+}$  concentration is observed for S3 sample only. The above is easy to explain under assumption that in „as grown“ S3 crystal  $Ce^{4+}$  ions are present.

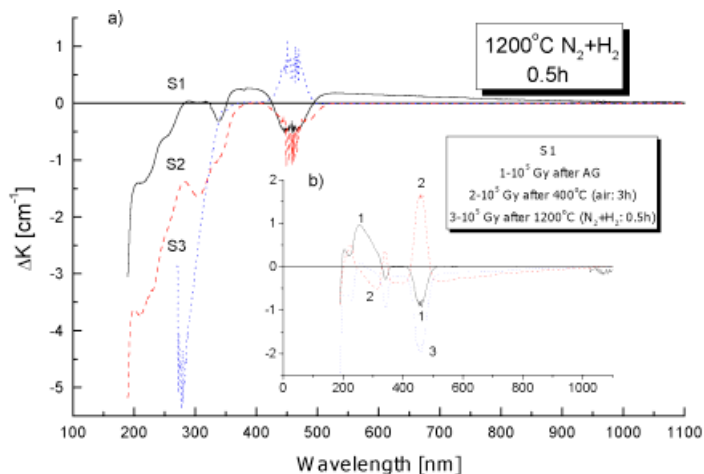


Fig. 3: AA bands for S1(YAG: Ce – 0.1 at. %), S2(YAG: Ce – 0.2 at. %) and S3(YAG: Ce, Mg – 0.2 at. % Ce, 0.1 at. % Mg) samples after annealing in reducing atmosphere (a) and  $\bullet$ -irradiation with a dose of  $10^5$  Gy of S1 sample (b)

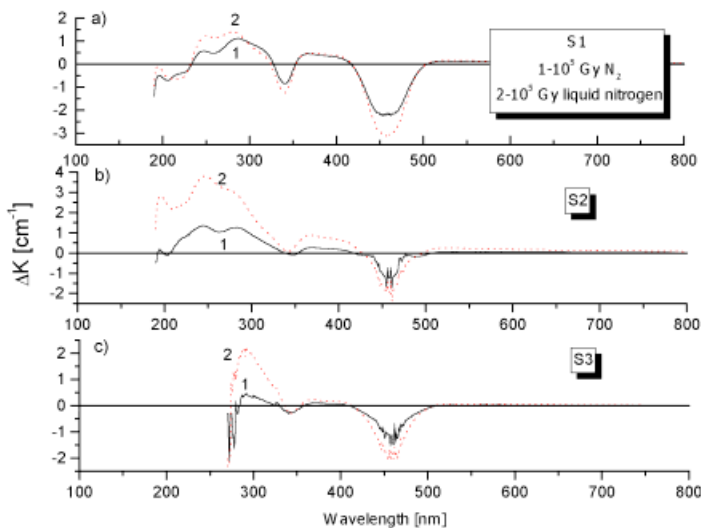


Fig. 4: AA bands for S1(YAG: Ce – 0.1 at. %), S2(YAG: Ce – 0.2 at. %) and S3(YAG: Ce, Mg – 0.2 at. % Ce, 0.1 at. % Mg) samples after  $\bullet$ -irradiation at 290K and 77K.

Fig. 3b shows changes in absorption spectrum for S1 sample after  $\gamma$ -irradiation. As one can see, the shape of the curve 1 is similar to AA band for the crystal after annealing in air (Fig. 2a). It suggests that in this case ionization processes take place. Further annealing of the crystal in air at 400°C and irradiation with the same  $\gamma$ -dose leads to opposite changes in AA picture. The irradiation with the same dose of  $\gamma$ -rays after annealing in reducing atmosphere gives the same type of AA as in Fig. 3a.

In Fig. 4 changes in AA spectra for S1...S3 samples after  $\gamma$ -irradiation performed at 77 K are compared to those at 300K. In the UV range changes are much greater than in VIS one.

Values of concentration of  $Ce^{3+}$  ions before and after  $\gamma$  or annealing treatments calculated from Smakula equation (DEXTER, KACZMAREK et al. 1997) are shown in the table. As is seen for small initial  $Ce^{3+}$  concentrations an increase in final concentration can reach even 50%. On the contrary, for concentrations higher than 0.05 at. % these changes are smaller, (less than 2%). In the case of small initial Ce concentration the calculations give somewhat lower values of cerium concentrations, as compared to those existing in the starting material. This fact can be explained by incomplete penetration of the Ce ions into the crystal (due to a small value of their distribution coefficient :  $\sim 0.07$ ), or by a not accurate enough estimation of the oscillator strengths for the transition.

Thus, under  $\gamma$  and proton irradiation as well as in thermal processing, a change of the concentration of  $Ce^{3+}$  ions takes place in Ce: YAG crystals having lower Ce content, as a result of recharging processes of the type  $Ce^{4+} \leftrightarrow Ce^{3+}$  at site positions (KACZMAREK, SUGAK et al. 1997). Observed changes in AA bands after  $\gamma$  or proton irradiation and their relative values suggest, that valency change in Ce: YAG crystals with higher Ce content can probably be attributed to the ionization of  $Ce^{3+}$  ions located at interstitial positions. The same refers to Mg, Ce: YAG crystal and  $Ce^{4+}$  ions existing in the crystal due to acceptor properties of  $Mg^{2+}$  ions.

The observed changes in luminescence spectrum appear to be correlated with positive or negative changes in AA spectrum (bands near 338 and 458 nm) of YAG crystal with cerium. We have observed changes as high as 100% for YAG (0.05 at. % Ce) and smaller (2%) for higher initial concentration of Ce.

Radiation and its dose	No.	K[cm <sup>-1</sup> ]	W[eV]	N <sub>Ce</sub> [at.%] before	N <sub>Ce</sub> [at.%] after	$\Delta N = [(N_{after} - N_{before}) / N_{before}] * 100\%$
Gamma quanta dose 10 <sup>5</sup> Gy	S1	45.33	0.237	0.1412	0.1387	-1.75
	S2	61.74	0.237	0.1923	0.1903	-1.05
	S3	58.4	0.237	0.1819	0.1855	1.96
	S4	2.3	0.237	0.0072	0.0102	41.77
Protons 10 <sup>13</sup> cm <sup>-2</sup> 3*10 <sup>13</sup> cm <sup>-2</sup> 10 <sup>14</sup> cm <sup>-2</sup> 10 <sup>15</sup> cm <sup>-2</sup>	S4	2.18	0.237	0.0068	0.0082	20.37
	S4	2.18	0.237	0.0068	0.0087	28.12
	S4	2.18	0.237	0.0068	0.0079	16.33
	S4	2.18	0.237	0.0068	0.0096	41.68

Table: Parameters of absorption spectrum of  $Ce^{3+}$  ions (K- absorption coefficient, W-half width of absorption band), with maximum at  $\lambda=458$  nm and calculated values of  $Ce^{3+}$  concentration (N<sub>Ce</sub>) and  $\Delta N$ -changes in N<sub>Ce</sub> for S1...S4 samples before and after  $\gamma$ - and proton irradiation with a dose of 10<sup>5</sup> Gy and fluency from 10<sup>13</sup> to 10<sup>15</sup> cm<sup>-2</sup>, respectively.

## 5. Conclusions

Defect structure of YAG single crystals doped with Ce clearly depends on the type of annealing atmosphere. Type of defects introduced into the crystals by irradiation process

strongly depend on the type of radiation and previous thermal treatment. Irradiation can improve some features of Ce: YAG crystals, changing, e.g., concentration of active dopant. Direction of these changes (an increase or a decrease) depends on the type of radiation and kind of thermal treatment.

For given type of irradiation an increase of the dose value (gamma's up to a dose of  $10^7$  Gy, protons up to a fluency of  $10^{15}$  cm<sup>-2</sup>) leads only to an increase in the density of created defects.  $\gamma$ -rays induce recombination of „as grown“ defects and ionization of defects left after annealing of the sample. For protons ionization by Coulomb field of the projectile and recombination by delta electrons produced along the proton trajectory are probably responsible for defect creation. In the case of protons with fluency greater than  $10^{14}$  cm<sup>-2</sup>, in interaction processes within the crystals, both ionization and Frenkel pair defects creation seem to be present.

### References

- AKHMADULIN, J.SH., MIGACHEV, S.A., MIRONOV, S.P.: Nuclear Instruments and Methods in Physics Research, **B65** (1992), 270
- DEXTER, D.L.: Phys. Rev., **101**(1) (1956) 48
- KACZMAREK, S.M., KISIELEWSKI, J., JABLONSKI, R., MOROZ, Z., KWASNY, M., LUKASIEWICZ, T., WARCHOL, S., WOJTKOWSKA, J.: Biuletyn WAT, **8** (1998) 56
- KACZMAREK, S.M., KWASNY, M., KISIELEWSKI, J., MOROZ, Z., MATKOVSKII, A.O., SUGAK, D.J.: Proc. SPIE, **3178** (1997) 279
- KACZMAREK, S.M., KWASNY, M., MALINOWSKI, M., MOROZ, Z.: Proc. of SPIE, **3186** (1997) 51
- KACZMAREK, S.M., KWASNY, M., MATKOVSKII, A.O., SUGAK, D.J., MIERCZYK, Z., FRUKACZ, Z., KISIELEWSKI, J.: Biuletyn WAT, **8** (1996) 93
- KACZMAREK, S.M., SUGAK, D.J., MATKOVSKII, A.O., MOROZ, Z., KWASNY, M., DURYGIN, A.N.: Nuclear Instruments and Methods in Physics Research **B132** (1997) 647
- KAMINSKII, A.A.: Laser crystals, Nauka, Moskwa 1975, 215
- SLACK, G.A., DOLE, S.L., TSOUKALA, V., NOLAS, G.S.: J. Opt. Soc. Am. **B11**(6) (1994) 961
- TOMIKI, T., AKAMINE, H., GUSHIKEN, M., KINJOH, Y., MIYAZATO, M., MIYAZATO, T., TOYOKAWA, N., HIRAOKA, M., HIRATA, N., GANAHA, Y., FUTEMMA, T.: J. Phys. Soc. Japan, **60**(7) (1991) 2437
- YEN, W.M., BASUN, S., HAPPEK, U., RAUKAS, M.: Acta Physica Polonica A, **90**(2) (1996) 257

(Received July 3, 1998; Accepted November 5, 1998)

### Authors' addresses:

dr S.M. KACZMAREK\*  
Institute of Optoelectronics, MUT  
2 Kaliski Str., 01-489 Warsaw, Poland

dr G. DOMINIAK-DZIK, prof. dr hab. W. RYBA-ROMANOWSKI  
Institute of Low Temperatures and Structure Research  
2 Okólna, 50-950 Wrocław, Poland

mgr J. KISIELEWSKI  
Institute of Electronic Materials Technology (ITME)  
133 Wólczyńska Str., 01-919 Warsaw, Poland

dr J. WOJTKOWSKA  
Soltan Institute of Nuclear Studies (SINS), 05-400 Swierk, Poland

\*corresponding author  
e-mail: skaczmar@wat.waw.pl